Nuclear Medicine and Biology 42 (2015) 780–787

Contents lists available at ScienceDirect

Nuclear Medicine and Biology

journal homepage: www.elsevier.com/locate/nucmedbio

A high-affinity [^{18} F]-labeled phosphoramidate peptidomimetic PSMA-targeted inhibitor for PET imaging of prostate cancer

Tanushree Ganguly [a,1], Shorouk Dannoon [b,1], Mark R. Hopkins [a], Stephanie Murphy [b], Hendry Cahaya [b], Joseph E. Blecha [b], Salma Jivan [b], Christopher R. Drake [b], Cyril Barinka [c], Ella F. Jones [b,2], Henry F. VanBrocklin [b,2], Clifford E. Berkman [a,d,*,2]

[a] Department of Chemistry, Washington State University, USA
[b] Department of Radiology and Biomedical Imaging, University of CA, San Francisco, USA
[c] Institute of Biotechnology, CR, Prague
[d] Cancer Targeted Technology, USA

ARTICLE INFO

Article history:
Received 19 March 2015
Received in revised form 26 May 2015
Accepted 3 June 2015

Keywords:
Flourine-18
PET
PSMA
Phosphoramidate

ABSTRACT

Introduction: In this study, a structurally modified phosphoramidate scaffold, with improved prostate-specific membrane antigen (PSMA) avidity, stability and *in vivo* characteristics, as a PET imaging agent for prostate cancer (PCa), was prepared and evaluated.
Methods: p-Fluorobenzoyl-aminohexanoate and 2-(3-hydroxypropyl)glycine were introduced into the PSMA-targeting scaffold yielding phosphoramidate 5. X-ray crystallography was performed on the PSMA/5 complex. [^{18}F]5 was synthesized, and cell uptake and internalization studies were conducted in PSMA(+) LNCaP and CWR22Rv1 cells and PSMA(−) PC-3 cells. *In vivo* PET imaging and biodistribution studies were performed at 1 and 4 h post injection in mice bearing CWR22Rv1 tumor, with or without blocking agent.
Results: The crystallographic data showed interaction of the *p*-fluorobenzoyl group with an arene-binding cleft on the PSMA surface. *In vitro* studies revealed elevated uptake of [^{18}F]5 in PSMA(+) cells (2.2% in CWR22Rv1 and 12.1% in LNCaP) compared to PSMA(−) cells (0.08%) at 4 h. *In vivo* tumor uptake of 2.33% ID/g and tumor-to-blood ratio of 265:1 was observed at 4 h.
Conclusions: We have successfully synthesized, radiolabeled and evaluated a new PSMA-targeted PET agent. The crystal structure of the PSMA/5 complex highlighted the interactions within the arene-binding cleft contributing to the overall complex stability. The high target uptake and rapid non-target clearance exhibited by [^{18}F]5 in PSMA(+) xenografts substantiates its potential use for PET imaging of PCa.
Advances in Knowledge: The only FDA-approved imaging agent for PCa, Prostascint®, targets PSMA but suffers from inherent shortcomings. The data acquired in this manuscript confirmed that our new generation of [^{18}F]-labeled PSMA inhibitor exhibited promising *in vivo* performance as a PET imaging agent for PCa and is well-positioned for subsequent clinical trials.
Implications for Patient Care
Our preliminary data demonstrate that this tracer possesses the required imaging characteristics to be sensitive and specific for PCa imaging in patients at all stages of the disease.

1. Introduction

Owing to its unique and ubiquitous expression in prostate cancers (PCa) with limited (100–1000 fold lower) expression in other organs, prostate-specific membrane antigen (PSMA) is an ideal biomarker [1] and has attracted significant attention as a target for imaging [2–7] and treatment of PCa [8–10].

The only FDA-approved single-photon emission computed tomography (SPECT) diagnostic imaging agent for PCa, Prostascint®, an ^{111}In-labeled antibody that recognizes an intracellular epitope of the PSMA transmembrane protein [11], is only accessible in damaged or necrotic prostate tumor cells. Even though other antibodies targeted to extracellular epitopes of PSMA have been employed successfully to deliver diagnostic and therapeutic radionuclides [3,12–14], the long accumulation and circulation times, poor tumor penetration, and multiple day imaging procedure result in their suboptimal diagnostic accuracy and reduced clinical use.

In contrast, small- molecule probes possess advantages of drug-like pharmacokinetics, high atom-economy, and reduced production costs. To point, Pomper et al. have pioneered the development of small

---

[*] Corresponding author at: Washington State University, Department of Chemistry, Pullman, WA 99164–4630. Tel.: +1 509 335 7613; fax: +1 509 335 8389.
E-mail address: cberkman@wsu.edu (C.E. Berkman).
[1] Contributed equally.
[2] Contributed equally as senior authors.

http://dx.doi.org/10.1016/j.nucmedbio.2015.06.003
0969-8051/© 2015 Elsevier Inc. All rights reserved.

molecule PSMA-targeted PET and SPECT probes to successfully image prostate tumor xenografts in mouse models, using a urea-based peptidomimetic scaffold with avidity for PSMA's active site [15–18]. While the pharmacokinetic and imaging profile with these agents appears more superior to antibody-based approaches, washout of the tracer over several hours was observed [15].

Recently, we demonstrated that our phosphoramidate-based peptidomimetic PSMA inhibitors may be outfitted with imaging payloads without having an adverse effect on their inhibitory capabilities [6,19]. Our lead irreversible phosphoramidate inhibitor 1, with a serine as the P1 residue and glutamate as the P1´ residue ($IC_{50} = 14$ nM) (Fig. 1) was modified to selectively deliver the tracer to PSMA(+) cells both *in vitro* and *in vivo*. When conjugated with a fluorescent dye, 1 was found to accumulate in PSMA(+) cells presumably through the internalization of the PSMA enzyme-inhibitor complex [19]. This phosphoramidate inhibitor 1 has also been validated for SPECT and PET imaging of with PSMA(+) cells and tumors when labeled with ^{99m}Tc and ^{18}F respectively [6,7,20].

In an effort to further our understanding of the phosphoramidate scaffold's binding to PSMA and to improve the overall *in vivo* characteristics for human use, we have structurally modified the scaffold with 2-(3-hydroxypropyl)glycine and aminohexanoate, forming a new phosphoramidate inhibitor 3 to improve its binding, stability and imaging efficacy. 3 was further appended with a [^{19}F]-fluorobenzoly moiety, yielding 5. Herein we report the synthesis, radiolabeling and characterization of [^{18}F]5 as well as its *in vitro* cell uptake and internalization in PSMA(+) LNCaP and CWR22Rv1 cells and PSMA(−) PC3 cells. Additionally, *in vivo* PET imaging and biodistribution data were obtained in mice implanted with CWR22Rv1 tumor xenografts.

2. Materials and methods

2.1. Cell lines, reagents and general procedures

LNCaP, CWR22Rv1 and PC-3 cells were obtained from the American Type Culture Collection (Manassas, VA). NCr-nu/nu mice (strain code 088) were purchased from Charles River (Hollister, CA). Z-6-Aminohexanoic acid (CBZ-AH-OH) was purchased from Sigma-Aldrich (St. Louis, MO). All chemicals and cell-culture reagents were purchased from Fisher Scientific (Sommerville, NJ) or Sigma-Aldrich. All solvents used in chemical reactions were anhydrous and obtained as such from commercial sources or distilled prior to use. All other reagents were used as supplied unless otherwise stated. Liquid flash chomatography (silica or C18) was carried out using a Flash Plus chromatography system (Biotage, Charlotte, NC). High-resolution mass spectrometry was performed using an ABS 4800 MALDI TOF/TOF Analyzer (Applied Biosystems, Framingham, MA). ESI was performed using API 4000 Electrospray Ionization Triple Quadrupole MS/MS. ^{1}H NMR chemical shifts were referenced to tetramethylsilane ($\delta = 0.00$ ppm), $CDCl_3$ ($\delta = 7.26$ ppm) or D_2O ($\delta = 4.87$ ppm). ^{13}C NMR chemical shifts were referenced to $CDCl_3$ ($\delta = 77.23$ ppm). ^{31}P NMR chemical shifts in $CDCl_3$ or D_2O were externally referenced to 85% H_3PO_4 ($\delta = 0.00$ ppm) in $CDCl_3$ or D_2O. Aqueous buffered solutions for *in vitro* experiments and HPLC chromatography were prepared with deionized distilled water (Milli-Q water system, Millipore, Billerica, MA).

The HPLC analysis and purification system for radioactive compounds were performed on a Waters model 600 Multisolvent System pump equipped with a Shimudzu model SPD-10A UV detector and an in-line radioactivity detector (model 105 s, Carroll and Ramsey Associates, Berkeley, CA) that was coupled to a data collection system (PeakSimple model 304, SRI, Torrance, CA).

2.2. Synthesis of phosphoramidate 3 and its fluorinated analogs

The general synthetic sequence of these compounds is shown in Fig. 2. Syntheses of precursors I and II, their intermediates, and *N*-succinimidyl-4-[^{18}F]fluorobenzoate ([^{18}F]SFB) and their supporting analysis data are provided in the Supplementary Information (Section 1).

2.2.1. 2-(((S)-((4R)-4-(4-(6-aminohexanamido)-4-carboxybutanamido)-4-carboxy but -oxy) (hydroxy)phosphoryl)amino)pentanedioic acid, 3

To a solution of a benzyl ester protected phosphoramidate (II) (0.160 g, 0.124 mmol) in THF (1 mL), was added 10% Pd/C (16 mg), K_2CO_3 (0.044 mg, 0.318 mmol) and H_2O (1 mL). The mixture was stirred vigorously, purged with $Ar_{(g)}$ and then charged with $H_{2(g)}$ under balloon pressure overnight at room temperature. The solution was filtered through a 0.2 μm PTFE micropore filtration disk (Whatman). The solvent was removed *in vacuo* to yield 3 as a white solid in 87% yield. ^{1}H NMR (300 MHz, D_2O): δ 1.23 (m, 3H), 1.48 (m, 6H), 1.74 (m, 4H), 1.80 (m, 1H), 1.98 (m, 4H), 2.15 (m, 4H), 2.86 (t, 4H), 3.34 (m, 1H), 3.56 (dd, 1H), 3.94 (m, 3H). ^{31}P NMR (300 MHz, D_2O): δ 8.42. HR mass spectroscopy: calculated 584.5, found 585.20 (M + H) for $C_{21}H_{37}N_4O_{13}P^{+}$.

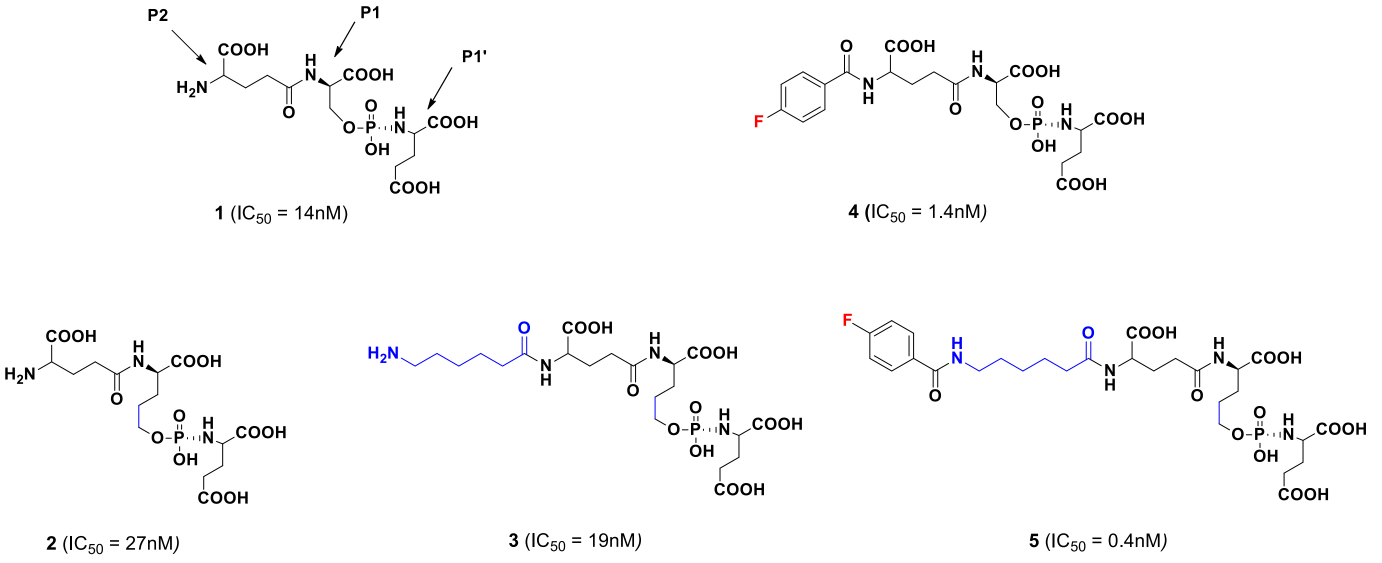

Fig. 1. Irreversible phosphoramidate analogs. The P1´, P1 and P2 residues for a typical phosphoramidate scaffold have been designated.